British Journal of Pharmacology

DOI:10.1111/j.1476-5381.2011.01532.x
www.brjpharmacol.org

RESEARCH PAPER

Plumbagin inhibits tumour angiogenesis and tumour growth through the Ras signalling pathway following activation of the VEGF receptor-2

Li Lai[1], Junchen Liu[1], Dong Zhai[1], Qingxiang Lin[1], Lijun He[1], Yanmin Dong[1], Jing Zhang[1], Binbin Lu[1], Yihua Chen[1], Zhengfang Yi[1] and Mingyao Liu[1,2]

[1]*Institute of Biomedical Sciences and School of Life Sciences, East China Normal University, 500 Dongchuan Road, Shanghai 200241, China, and* [2]*Center for Cancer and Stem Cell Biology, Institute of Biosciences and Technology and Department of Molecular and Cellular Medicine, Texas A&M University Health Science Center, Houston, Texas 77030, USA*

Correspondence
Zhengfang Yi and Mingyao Liu, Institute of Biomedical Sciences, East China Normal University, 500 Dongchuan Road, Shanghai 200241, China. E-mail: ibms.ecnu@gmail.com

Keywords
plumbagin; tumour angiogenesis; VEGFR2; Ras pathway

Received
14 January 2011
Revised
24 May 2011
Accepted
31 May 2011

BACKGROUND AND PURPOSE

Angiogenesis-based therapy is an effective anti-tumour strategy and previous reports have shown some beneficial effects of a naturally occurring bioactive compound plumbagin (5-hydroxy-2-methyl-1, 4-naphthoquinone). Here, we sought to determine the biological effects of plumbagin on signalling mechanisms during tumour angiogenesis.

EXPERIMENTAL APPROACH

The effects of plumbagin were evaluated in various *in vitro* assays which utilised human umbilical vein endothelial cells (HUVEC) proliferation, migration and tube formation. Plumbagin was also evaluated *in vivo* using chicken embryo chorioallantoic membrane (CAM) and mouse corneal micropocket models., Human colon carcinoma and prostate cancer xenograft mouse models were used to evaluate the effects of plumbagin on angiogenesis. Immunofluorescence, GST pull-down and Western blotting were employed to explore the underlying mechanisms of VEGF receptor (VEGFR)2-mediated Ras signalling pathways.

KEY RESULTS

Plumbagin not only inhibited endothelial cell proliferation, migration and tube formation but also suppressed chicken chorioallantoic membrane neovascularzation and VEGF-induced mouse corneal angiogenesis. Moreover, plumbagin suppressed tumour angiogenesis and tumour growth in human colon carcinoma and prostate cancer xenograft mouse models. At a molecular level, plumbagin blocked the Ras/Rac/cofilin and Ras/MEK signalling pathways mediated by VEGFR2 in HUVECs.

CONCLUSIONS AND IMPLICATIONS

Plumbagin inhibited tumour angiogenesis and tumour growth by interference with the VEGFR2-mediated Ras signalling pathway in endothelial cells. Our findings demonstrate a molecular basis for the effects of plumbagin and suggest that this compound might have therapeutic ant-tumour effects.

Abbreviations

HUVEC, human umbilical vein endothelial cells; CAM, chicken embryo chorioallantoic membrane; TCMM, Traditional Chinese Materia Medica; vWF, von Willebrand Factor; IOD, integrated optical density; MEK, mitogen-activated ERK kinase; LIMK, LIM domain kinase; PAK, p21 activated kinase

Introduction

Angiogenesis, the sprouting or intussusception of parent blood vessels to form new ones (Carmeliet and Jain, 2000), is a characteristic of malignant neoplasia development (Eikesdal *et al.*, 2008) and therapy based on blocking such angiogenesis has been shown to be an effective strategy in inhibiting tumour growth and metastasis (Cho *et al.*, 2009).A major pro-angiogenic cytokine is vascular endothelial growth factor (VEGF) which comprises several isotypes, including VEGF (VEGF-A, vascular permeability factor), VEGF-B, VEGF-C and VEGF-D, as numerous splice variant isoforms. VEGF-A and VEGF-B promote vascular angiogenesis primarily through activation of two receptors, VEGFR-1 (Flt1) and VEGFR-2 (Flk1/KDR) (Huang *et al.*, 2007) and VEGFR2 inhibitors have licensed for the treatment of tumours (Cabebe and Wakelee, 2006; Kane *et al.*, 2006).

In VEGF/VEGFR2-mediated intracellular signalling pathways, the small guanine nucleotide-bound protein Ras (21 kDa) plays a multifaceted role in tumour angiogenesis and tumour growth (Rak and Kerbel, 2001). In endothelial cells, following stimulation by VEGF, GDP-bound inactive Ras is transformed to the GTP-bound active Ras (Meadows *et al.*, 2001). The GTP-bound Ras activates a number of angiogenic signalling pathways such as the Rac and MEK pathways (Dancey, 2002), which ultimately control processes critical to angiogenesis such as endothelial cell proliferation (Meadows *et al.*, 2004), migration (Kranenburg *et al.*, 2004) and branching morphogenesis (Meadows *et al.*, 2001) Increased Ras activity can be frequently detected in human cancers because of genetic mutations and amplification (Hoa *et al.*, 2002). Mutations of activated oncogenic Ras genes comprising H-Ras, K-Ras and N-Ras have a wide-ranging influence in tumour genesis, tumour malignancy and progression (Bos *et al.*, 1987; Parikh *et al.*, 2007). Recently, a number of agents such as R115777 and SCH 66336 that disrupt Ras activity and its downstream proteins have entered clinical trials (Hanrahan *et al.*, 2009; Karp *et al.*, 2009). Hence, Ras signalling pathways are deemed as important targets for anticancer therapies (Morgan *et al.*, 2007).

Natural products such as those included in the Traditional Chinese Materia Medica (TCMM) represent a rich resource of compounds for drug discovery and the TCMM is currently being explored for agents to target tumour angiogenesis (Neal *et al.*, 2006; Yi *et al.*, 2008a,b; Pang *et al.*, 2009). Plumbagin (5-hydroxy-2-methyl-1,4-naphthoquinone) is a naturally occurring, biologically active compound isolated from Chinese medicinal plants such as the Plumbaginaceae, Droseraceae and Ebenaceae (Sandur *et al.*, 2006). Earlier studies have demonstrated anticancer (Krishnaswamy and Purushothaman, 1980), anti-fertility (Premakumari *et al.*, 1977), anticoagulant (Santhakumari *et al.*, 1978) and antibacterial properties (Krishnaswamy and Purushothaman, 1980; Dzoyem *et al.*, 2007) for plumbagin. Later reports also demonstrated that it exerted gonadotrophic (Saxena *et al.*, 1996), hypolipidaemic and anti-atherosclerotic effects (Sharma *et al.*, 1991). Furthermore, recent research indicated that plumbagin also possessed anti-mite (Lee and Lee, 2008), and anti-inflammatory activity (Checker *et al.*, 2009) and had beneficial effects in experimental cerebral ischaemia (Son *et al.*, 2010). Nevertheless, to our knowledge, little information has been reported on the effects and molecular mechanisms of plumbagin in tumour angiogenesis.

In this study, we have identified plumbagin as a novel inhibitor of tumour angiogenesis and characterized its underlying molecular mechanisms. The anti-angiogenenic properties of plumbagin were evaluated *in vitro* using human umbilical vein endothelial cell (HUVEC) proliferation, migration and tubular formation assays and *in vivo* by chick embryonic chorioallantoic membrane (CAM) assay and mouse corneal micropocket assay models. Moreover, we demonstrated that plumbagin suppressed human colon and prostate tumour growth in xenograft mouse models via inhibition of tumour angiogenesis. At a molecular level we showed that plumbagin inhibited angiogenesis by blocking the VEGFR2-mediated Ras/Rac/cofilin and Ras/MAPK signalling pathways in endothelial cells.

Methods

Migration and tubulogenesis assays

HUVECs were purchased from ScienCell Research Laboratories and cultured in ECM (ScienCell, Carlsbad, CA, USA). Using our previously described methods (Yi *et al.*, 2008b), we estimated the inhibitory activity of plumbagin on HUVEC migration by using scratching and Boyden chamber migration assays. First, equal nembers of HUVECs were seeded in six-well plates pre-coated with 0.1% gelatin (Sigma, Shanghai, China). The cells were grown to confluence, starved overnight and then scratched with pipette tips and washed with PBS. Then the cells were treated with 4 $ng \cdot mL^{-1}$ VEGF and, in the absence or presence of different concentrations of plumbagin; 8–10 h later, the migration states of the cells were photographed using an Olympus inverted microscope, and the migrated cells were quantified. For the Boyden chamber migration assay, HUVECs (4×10^4 cells per well) were seeded into upper chambers of the 8 μm pore sized transwells (Millipore), and the lower chambers were filled with medium containing 4 $ng \cdot mL^{-1}$ VEGF as the stimulus. At the same time, cells were treated with varied concentrations of plumbagin. After 4 h of migration, cells were fixed with 4% formaldehyde and stained with haematoxylin and eosin (H&E). Cells that had migrated to the down surface of the transwell were photographed with the Olympus inverted microscope and then quantified.

Endothelial cell tubulogenesis assays were performed as previously described (Yi *et al.*, 2009). Briefly, Matrigel was defrosted at 4°C overnight, and each chilled well of a 24-well plate was coated with 120 μL Matrigel and then incubated at 37°C for 30 min. Afterwards, 5×10^4 HUVECs were seeded into each well in the presence of increasing concentrations of plumbagin. The capillary structures formed in the subsequent 8–10 h, were then recorded by the inverted microscope and quantified.

CAM assay

Fertilized chicken eggs were purchased from Shanghai Poultry Breeding Co. Ltd. (Shanghai, China). Fertilized chicken eggs were incubated in the constant temperature of 37°C and humidity of 60% for 3 days. Then a 1–2 cm^2 sized

window was carefully opened on the top of the air chamber in the eggs, and the shell membrane was cautiously lifted to expose the chorioallantoic membrane (CAM) (Cho *et al.*, 2009). Then sterilized filter papers impregnated with vehicle or various concentrations of plumbagin and hydrocortisone, were placed on the CAM.The windows were then sealed with cellulose tape to prevent infection. Five days later, the windows were opened in order to determine the extent of the neovascularisation around the filter paper, and Image-Pro Plus 6.0 software was utilised in the final statistical analysis.

Mouse corneal angiogenesis assay

All animal care and experimental protocols were approved by the Animal Investigation Committee of East China Normal University. C57BL/6 and nude mice were obtained from the Animal Center of Chinese Academy of Science. VEGF slow-releasing micro-pellets (0.35 × 0.35 mm), consisting of a mixture of sucralfate, hydron poly(hydroxyethylmethacrylate) (poly HEMA, Sigma) and 160 ng VEGF, were prepared. Under anaesthesia, the corneas of one eye of C57BL/6 mice were carefully opened with a modified pinhead to form micropockets. Into each micropocket was implanted grains containing VEGF as detailed in a previous study (Kenyon *et al.*, 1996; Cho *et al.*, 2009). For the next four days the mice received (by i.p. injection) either 10 $mg{\cdot}kg^{-1}$ day^{-1} plumbagin or DMSO . After this time, the images of the mice corneas were photographed by an Olympus stereo microscope. The following formula was used to calculate the growth area of neovascularization. Area (mm^2) = 0.2 × 3.14 × VL × CN, where VL is the maximal vessel length extending from the limbal vasculature towards the pellet, CN is the clock hours of neovascularization and 1 clock hour equals 30 degrees of arc (Kenyon *et al.*, 1996; Cho *et al.*, 2009).

Cell proliferation assay

HCT116 human colorectal carcinoma cells and PC-3 human prostate cancer cells were from the American Type Culture Collection (Manassas, VA, USA) and cultured in 1640 medium supplemented with 10% FBS and 1% antibiotics. Cell MTS viability assays were performed as described (Yi *et al.*, 2009). Briefly, HUVEC, HCT116 or PC-3 cells were seeded into 96-well plates (5×10^3 cells per well) and exposed to different concentrations of plumbagin for about 72 h before CellTiter 96® AQueous One Solution Reagent (Promega, Madison, WI, USA) (20 µL·per well) was added for a further 3 h. After that, the cell proliferation was assessed by measuring the light absorption value at the wavelength of 490 nm using a Spectra Max 190 microplate-reader (Molecular Devices, Sunnyvale, CA, USA). Cell BrdU incorporation assay was performed with the following protocol; 20,000 cells of HUVEC, HCT116 or PC-3 were implanted into 24-well plates and were treated with vehicle or 3 µM plumbagin for 24 h. BrdU was added into the cell medium to a final concentration of 200 µM for 2 h before the cells were fixed, denatured and blocked with 5% FBS. The cells were then incubated with anti-BrdU antibody at 4°C overnight and Alexa Fluor 488 s-antibody for 1 h as well as 4′,6-diamidino-2-phenylindole (DAPI) for 10 min. Images were taken by an Olympus inverted microscope.

Xenograft tumour growth assay and immunohistochemistry

PC-3 cells or HCT116 cells were injected s.c. (7×10^6 HCT116 cells or 3×10^6 PC-3 cells per mouse) into nude mice as previously reported (Yi *et al.*, 2009). When the average volume of tumours reached about 150 mm^3 for HCT 116 and 60 mm^3 for PC-3, respectively, mice received intralesional injection either with plumbagin (6 $mg{\cdot}kg^{-1}{\cdot}day^{-1}$ for HCT116 group and 10 $mg{\cdot}kg^{-1}{\cdot}day^{-1}$ for PC-3 group) or DMSO alone every day for 20 days. During the administration of plumbagin, the body weight and the tumour size of the mice were monitored every 2 days. The tumour volume was calculated using the following equation: volume = (length) × $(width)^2$ × 0.52 (Dong *et al.*, 2010). The mice were killed, and the tumours were isolated, photographed, weighed, fixed and embedded in paraffin. The 5 µm paraffin sections then were prepared and stained with blood vessel specific antibody against the von Willebrand Factor (vWF). The immunohistochemistry pictures were obtained by Leica Upright Metallurgical Microscope. The IOD (integrated optical density) value of the blood vessels was calculated by Image-Pro Plus 6.0 software.

F-actin staining and immunofluorescence analysis

F-actin detection was performed as previously described (Kobayashi *et al.*, 2006). HUVECs were seeded on glass cover slips pre-coated with 0.01% polylysine. The cells were treated with or without 5 µM plumbagin for 0.5 h and then were stimulated with 200 $ng{\cdot}mL^{-1}$ VEGF for 15 min. Then the cells were fixed in 4% paraformaldehyde for 20 min at room temperature and were permeabilized with 0.1% Triton X-100 for 15 min at room temperature followed by washing three times with PBS. Actin filaments were stained by phalloidin-FITC for 20 min, and nuclei were detected by DAPI. For phosphor-cofilin immunofluorescence, cells were blocked with 5% BSA in PBS for 1 h at 37°C. After washing three times with PBS, cells were incubated with antibody against phospho-cofilin, overnight at 4°C and then with secondary antibodies for another 1 h at room temperature. Next, cell nuclei were stained by DAPI for 10 min. The slides were processed for Leica confocal laser scanning microscopy.

GST-PBD pull-down assay

The GTPase activity of Ras and Rac1 was measured by GST-RBD or GST-PBD pull-down assays as described (Pang *et al.*, 2009). HUVECs were starved overnight and treated with different concentrations of plumbagin for 2 h and then stimulated with 200 $ng{\cdot}mL^{-1}$ VEGF for 0.5 h. Cells were harvested in Mg^{2+} lysis/wash buffer (25 mM HEPES, pH 7.5, 150 mM NaCl, 1% Igepal CA-630, 10 mM $MgCl_2$, 25 mM sodium fluoride, 1 mM sodium orthovanadate, 1 mM EDTA and 2% glycerol). About 500 µg protein extracts were incubated with 30 µg GST fusion protein bound to glutathione-sepharose beads for 1 h at 4°C. Active Ras and RhoA were precipitated with GST-RBD and active Rac1 were precipitated with GST-PBD. The active Ras, Rac1 and RhoA were analysed by Western blotting using specific antibodies against Ras Rac1 and RhoA.

Western blotting

Cells were starved overnight and then incubated with plumbagin for 2 h. Subsequently, the cells were stimulated with 200 ng·mL^{-1} VEGF for 10 min. Western blotting assays were performed with specific antibodies. Anti-mouse IgG and anti-rabbit IgG (Molecular Probes) labelled with fluorescence as the secondary antibodies were used to detect Western blotting with LI-COR Odyssey scanner.

Statistical analysis

Data are presented as the mean ± SD of three independent experiments, and statistical comparisons were based on two tailed Student's *t*-test or analysis of variance. A probability value of 0.05 was considered to be statistically significant.

Materials

Plumbagin was obtained from Sigma with a purity of more than 98%. VEGF was from R&D Systems (Minneapolis, MN, USA). Matrigel was from BD Biosciences (Pasadena, CA, USA). Antibodies (anti-p21 activated kinase-1 (PAK1), anti-MEK1/2, anti-ERK, anti-JNK, anti-cofilin, anti-LIM domain kinase-1 (LIMK1), anti-phospho-PAK1, anti-phospho-MEK1/2, anti-phospho-ERK, anti-phospho-JNK, anti-phospho-cofilin and anti-phospho-LIMK1) were purchased from Cell Signaling Technology (Danvers, MA, USA). Anti-Rac1 antibody was from Millipore (Billerica, MA, USA). BrdU and anti-BrdU antibody were from Sigma. Alexa Fluor® 488 Dye secondary antibody was from Invitrogen (Carlsbad, CA, USA). All drug and molecular target nomenclature follows Alexander *et al.*, (2011).

Results

Plumbagin inhibits VEGF-induced HUVEC migration and capillary-like structure formation in vitro

Endothelial cell migration is one of the most important steps in the process of angiogenesis. To assess the effects of plumbagin on HUVEC migration, we examined HUVEC migration in horizontal and vertical planes using the scratching and Boyden chamber assays. When HUVEC migration was stimulated with 4 ng·mL^{-1} VEGF, the number of migrated cells treated with 5 μM plumbagin was much less than that of control (VEGF alone) (Figure 1B and C). Our results demonstrated that plumbagin caused strong inhibition of VEGF-induced HUVEC migration, in a dose-dependent manner.

HUVECs can also spontaneously form capillary-like structures on Matrigel and so we studied the effects of plumbagin on tubulogenesis in HUVECs. Our data showed that the number and the continuity of HUVEC capillary-like structures were all dramatically inhibited by 0.1–5 μM plumbagin in a dose-dependent manner (Figure 1D), suggesting that plumbagin inhibited HUVEC tube formation *in vitro*.

Plumbagin inhibits angiogenesis in vivo

In order to determine whether plumbagin affects neomicrovessel growth *in vivo*, we performed chicken CAM and mouse corneal micropocket assays. In the CAM assay, the fertilized chicken eggs formed blood vessels, especially microvessels (Figure 2A, arrows). As shown in Figure 2A, plumbagin reduced the number of microvessels at both 5 μg·per disc and 15 μg·per disc demonstrating that plumbagin inhibited CAM angiogenesis.

For futher evaluation of the effects of plumbagin on angiogenesis *in vivo*, we used the mouse corneal micropocket model. Under normal conditions, there are no visible blood vessels in the cornea. Administration of 160 ng VEGF induces blood vessels to grow upwards into the cornea from the corneoscleral limbus (Figure 2B, green arrows). However, VEGF- induced corneal angiogenesis was significantly reduced in mice receiving plumbagin (10 mg·kg^{-1} day^{-1} i.p. for 4days ; Figure 2B) Statistical analysis of the results showed that plumbagin suppressed angiogenesis in the mouse corneal micropocket assay as indicated by three parameters including vessel length, clock number and area (Figure 2C).

Plumbagin inhibits tumour angiogenesis and tumour growth in xenograft mouse models

Tumour growth depends on angiogenesis and in order to evaluate the effects of plumbagin on tumour angiogenesis *in vivo*, we used human colon carcinoma (HCT116) and prostate cancer (PC-3) xenograft mouse models. Our results showed that after a 20 day treatment with plumbagin (6 mg·kg^{-1} day^{-1} for HCT116 group and 10 mg·kg^{-1} day^{-1} for PC-3 group, respectively), both tumour volume (Figure 3A and B) and tumour weight (Figure 3C) in treated groups were significantly less than those in the control group. In addition, in these experiments there were no notable side effects, such as weight loss, found in either groups of tumour-bearing mice (Figure 3D), suggesting that effective doses of plumbagin inhibited tumour growth with lfew side effects.

For further studies on the effects of plumbagin on tumour angiogenesis, we performed immunohistochemistry staining on the 5 μm paraffin sections with blood vessel specific antibody of vWF. As shown in Figure 4A–C, the cellular structure density and the IOD value of tumour blood vessels (arrows) in plumbagin-treated tumours (right panel of Figure 4A and B) were significantly less than that in the control group (left panel of Figure 4A and B) in both HCT116 and PC-3 xenograft tumours. For comparison of the effects of plumbagin on proliferation of endothelial cells and tumour cells, we also performed MTS assays and BrdU incorporation assays in HUVECs, HCT116 cells and PC-3 cells. As shown in Figure 4D, plumbagin impeded HUVEC and tumour cell (HCT116 and PC-3) proliferation in a dose-dependent manner. HUVECs were more sensitive to plumbagin (IC_{50} < 5 μM) than tumour cells (HCT116 and PC-3 cells, IC_{50} > 5 μM). Moreover, from data shown in Figure S1, it can be seen that upon treatment of the different cells with 3 μM plumbagin for 24 h, BrdU-positive cells were scarcely found in HUVECs, whereas the BrdU-positive ratio is much higher in the other two cell types, indicating that the proliferation of HUVEC was more sensitive to the plumbagin treatment than that of HCT16 and PC-3 cells.

Plumbagin suppresses VEGF-induced stress fibre formation via the VEGFR2-mediated Ras/Rac1/cofilin pathway in HUVECs

Our results demonstrated that plumbagin reduced cell migration (Figure 1B and C), and therefore we decide to evaluate

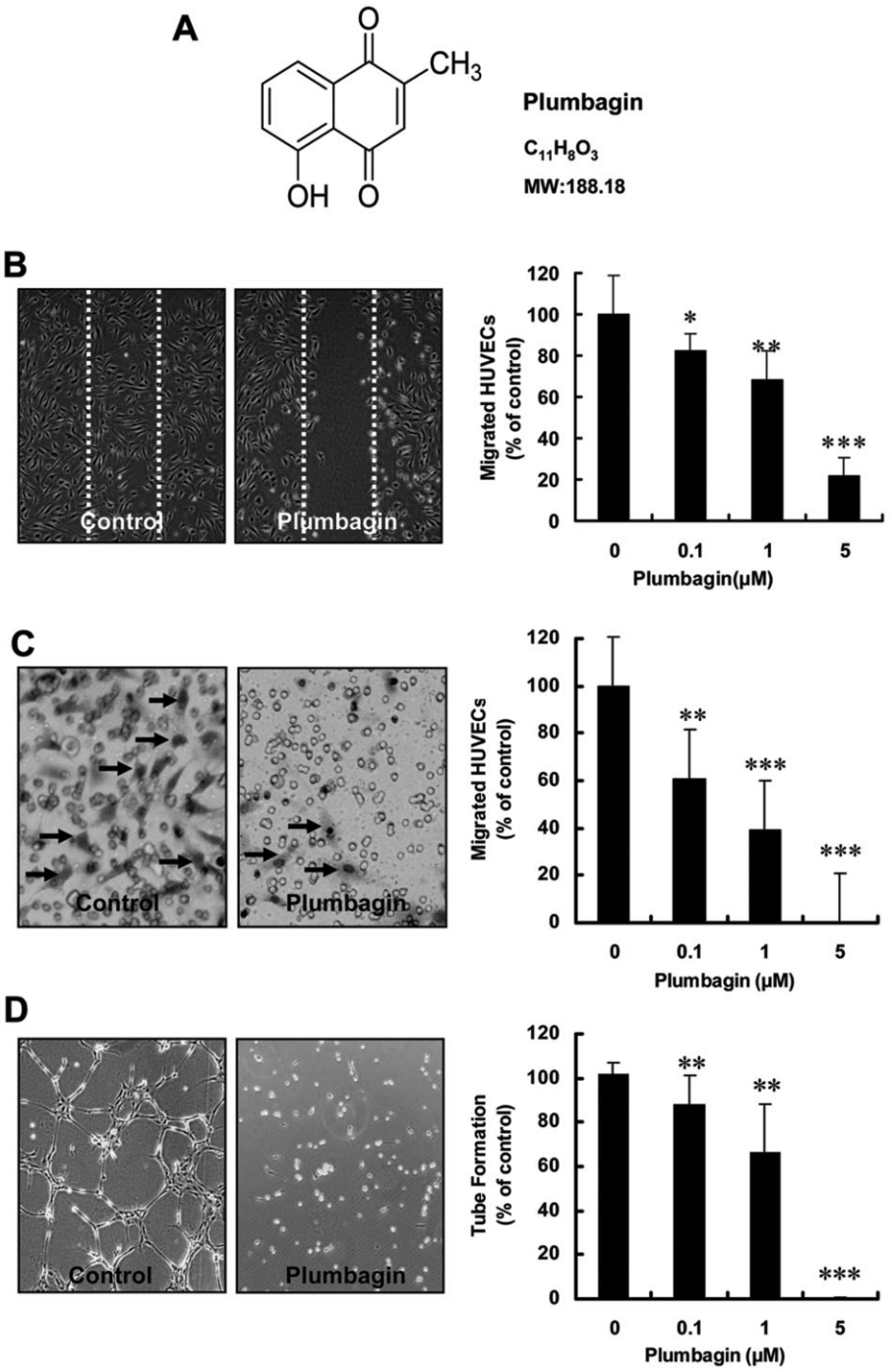

Figure 1

Plumbagin inhibited HUVEC migration and tube formation. (A) The chemical structure of plumbagin (MW 188). (B) The effect of plumbagin on HUVEC migration in scratch assay. HUVECs were treated with indicated concentrations of plumbagin with 4 ng·mL^{-1} VEGF after growing into confluency. Representative photomicrographs of cells treated with 4 ng·mL^{-1} VEGF (control) or VEGF together with 5 μM plumbagin were shown in the left panel. The area between the two dotted lines was the initial scraping (*$P < 0.05$; **$P < 0.05$; ***$P < 0.001$). (C) Plumbagin suppressed HUVEC migration in transwell assay. HUVECs (4×10^4 cells per well) were seeded into the transwells and then incubated with 4 ng·mL^{-1} VEGF and different concentrations of plumbagin. Cells were allowed to migrate for 4 h. HUVECs treated with VEGF alone, and 5 μM plumbagin were represented. The cells marked by arrows were the ones that migrated to the lower surface of the transwell (**$P < 0.05$; ***$P < 0.001$). (D) Plumbagin inhibited HUVEC tube formation. HUVECs were seeded into the 24-well plate pre-coated with Matrigel, then treated with different concentrations of plumbagin or DMSO alone. The capillary structures were examined by Olympus microscope after 6–8 h, and statistical analysis was performed by Image-Pro Plus software. HUVECs treated with DMSO alone, and 5 μM plumbagin are shown (magnification 100×; **$P < 0.05$; ***$P < 0.001$).

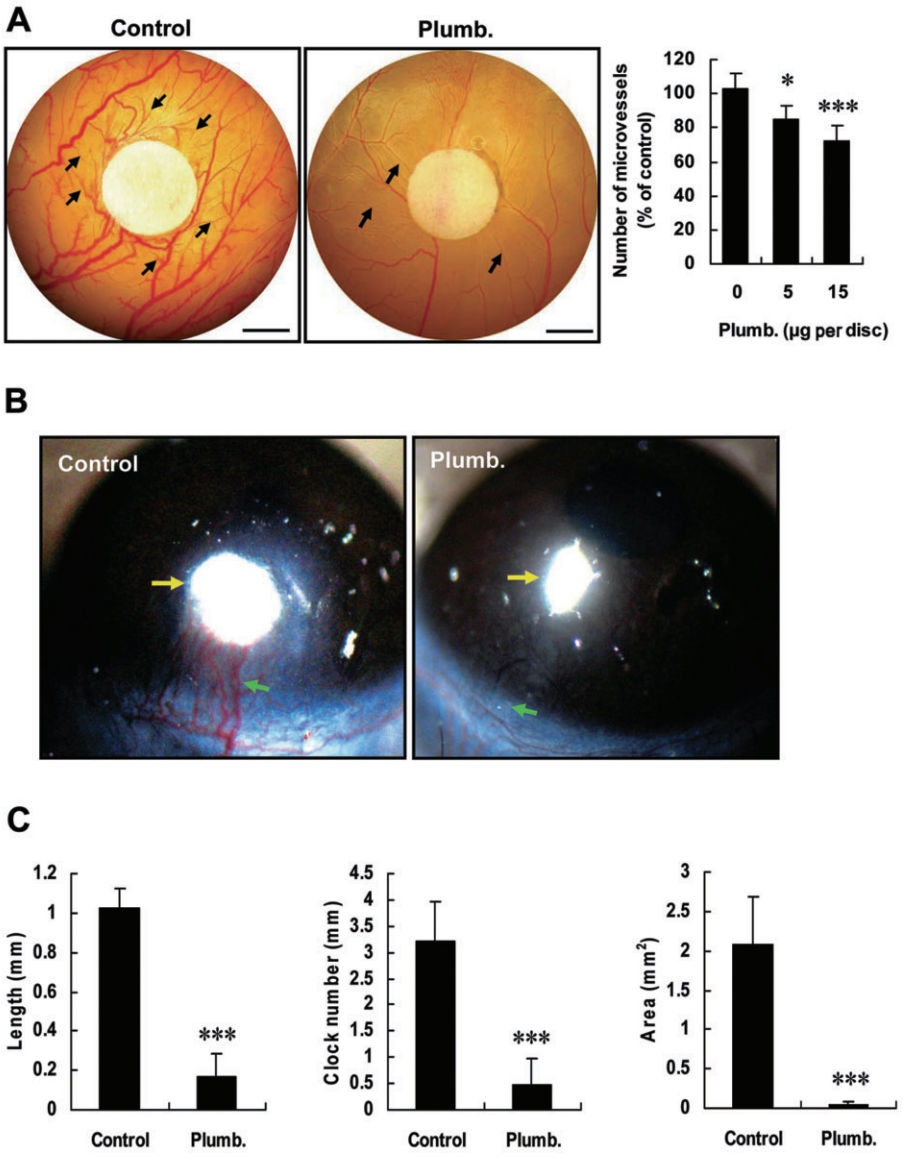

Figure 2

Pumbagin inhibited VEGF-induced angiogenesis *in vivo*. *A*, Plumbagin inhibited angiogenesis in the chicken chorioallantoic membrane (CAM) assay. The central circular filters contained various concentrations of plumbagin (Plumb). The representative photographs of control and 15 μg·per disc plumbagin-treated CAMs were shown. Arrows point to new capillary vessels (bar = 3 mm). The number of the microvessels was quantified in the right histogram ($n \geq 5$, $^{*}P < 0.05$; $^{***}P < 0.001$). *B*, Plumbagin suppressed VEGF-stimulated angiogenesis in mouse corneal micropocket assay. The micropellets (yellow arrows) containing 160 ng VEGF, aluminum and poly HEMA were implanted into corneal micropockets. Mice were intraperitoneally treated with the dosage of 10 $mg \cdot kg^{-1}$ day^{-1} plumbagin (Plumb) for 4 days after pellet implantation. The green arrow indicates the VEGF-induced microvessels in corneal. *C*, Statistical results for the inhibitory effect of plumbagin on corneal micropocket assay shown in three different parameters, consist of vessel length, clock number and vessel area (Area = 0.2 × 3.14 × Vessel Length × Clock Number, $n = 5$; $^{***}P < 0.001$).

this effect in more detail. Accordingly, we investigated the effects of plumbagin on cell cytoskeleton and stress fibre formation which are key cellular events involved in cell migration. Confocal image analysis of individual cells revealed that VEGF caused a robust induction of stress fibre formation which was inhibited by 5 μM plumbagin (Figure 5A). As activation of cofilin is an essential component of actin polymerization and depolymerization, and significantly affects cell cytoskeleton reorganization, we next examined the effects of plumbagin on VEGF-induced phosphorylation of cofilin using immunofluorescence techniques. Results shown in Figure 5B demonstrate that 5 μM plumbagin reduced VEGF-induced cofilin phosphorylation and activation, suggesting that the compound inhibited HUVEC migration by affecting cofilin activity and cell stress fibre formation.

VEGF-driven actin-based motility is mediated by VEGFR2 in endothelial cells (Rousseau *et al.*, 2000), and so we specu-

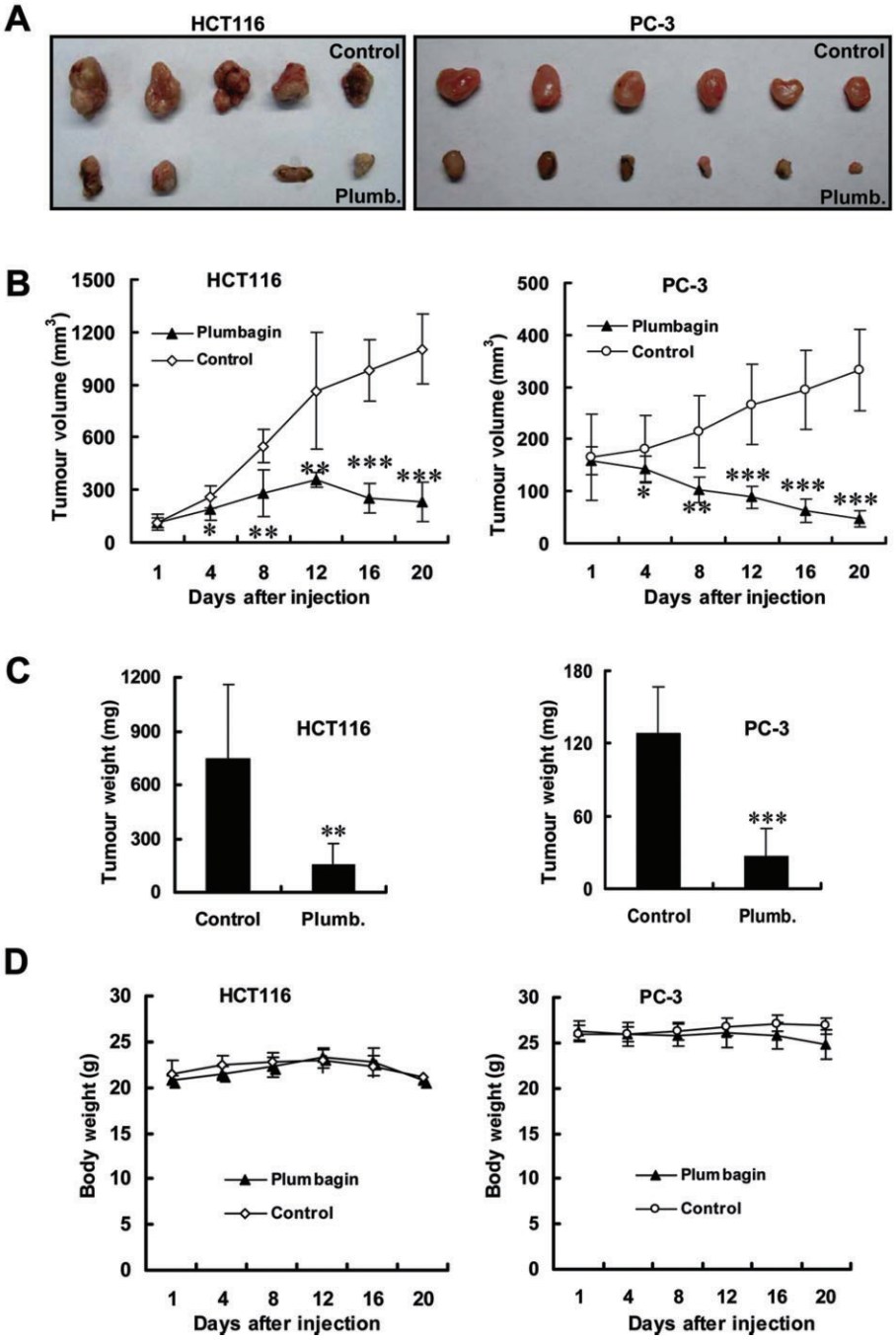

Figure 3

Plumbagin inhibited colon (HCT116) and prostate (PC-3) tumour growth with low side effects in the xenograft mouse tumour models. (A) Representative photos of HCT116 (left panel, $n = 5$) and PC-3 (right panel, $n = 6$) tumours removed from mice at day 20 after different treatment of intralesional administration (6 mg·kg^{-1} day^{-1} for HCT116 tumours and 10 mg·kg^{-1} day^{-1} for PC-3 tumours respectively). (B) Summary results of the HCT116 (left panel) and PC-3 (right panel) tumour volume in control group and plumbagin-treated group (*$P < 0.05$; **$P < 0.01$; ***$P < 0.001$). (C) Average weight of the HCT116 and PC-3 tumours in the xenograft model in control group and plumbagin-(Plumb) treated group (**$P < 0.01$; ***$P < 0.001$). (D) Records of the mouse body weight during the treatment of plumbagin on HCT116 and PC-3 tumours.

lated that plumbagin might influence VEGF-induced VEGFR2 activity. In order to test this hypothesis, we assessed the phosphorylation level of VEGFR2 in HUVECs by Western blotting. As expected, plumbagin limited VEGF-induced phosphorylation of VEGFR2 in a dose-dependent manner (Figure 5C).

Our next series of experiments were aimed at investigating the effects of plumbagin on events downstream of

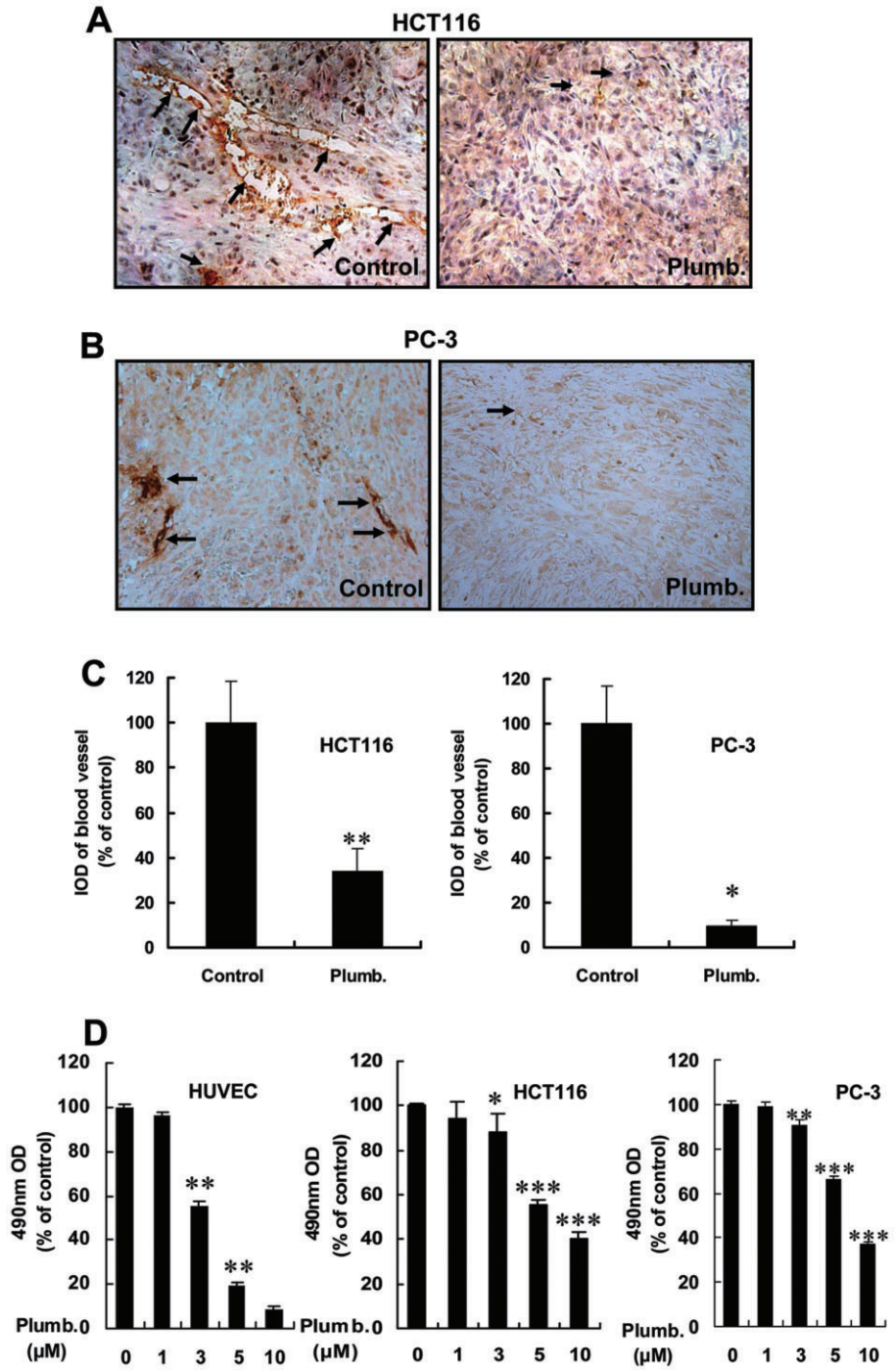

Figure 4

Plumbagin inhibited HCT116 and PC-3 tumour angiogenesis. (A) HCT116 tumour sections of control (left panel) and plumbagin-treated group (Plumb ; right panel) were immunostained for vWF (arrows point to the microvessels, magnification 100×). (B) Immunohistochemistry of paraffin sections (5 μm) of the PC-3 tumours stained with anti-vWF antibody. (C) Summary results of the blood vessel IOD in the HCT116 and PC-3 tumour immunohistochemistry analysed by Image-Pro Plus software (*$P < 0.05$; **$P < 0.01$). (D) Statistical results of MTS proliferation assays of plumbagin on HUVECs, HCT116 and PC-3 cells (*$P < 0.05$; **$P < 0.01$; ***$P < 0.001$).

VEGFR2 signalling, focussing on the small GTPases, such as Ras, RhoA and Rac1. Our GST pull-down result revealed that plumbagin resulted in suppression of VEGF-induced activation of both Ras and Rac1 (GTP-bound forms) but did not significantly affect the activity of RhoA. Furthermore, the phosphorylation and activation of downstream proteins of Rac1, such as PAK1, LIMK1 and cofilin, were all reduced by plumbagin in a dose-dependent manner (Figure 5D). Taken

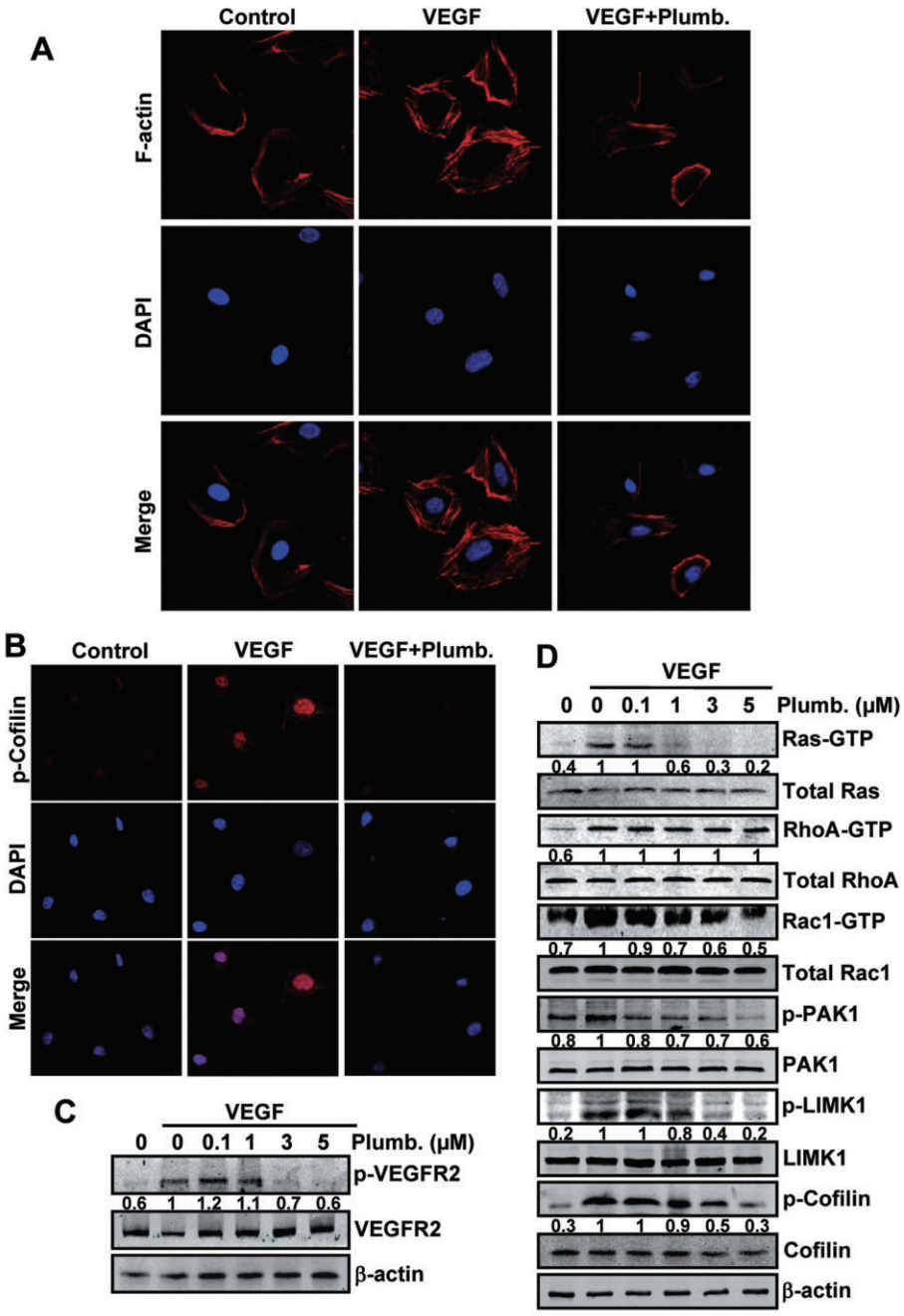

Figure 5

Plumbagin inhibited VEGF-induced stress fibre formation via the VEGFR2-mediated Ras/Rac signalling pathway. (A) Confocal images showed that plumbagin suppressed VEGF-induced stress fibre formation in endothelial cells. HUVECs were exposed to 5 μM plumbagin (Plumb) for 0.5 h and then were stimulated with or without VEGF for 15 min. F-actin of cells was visualized by phalloidin-FITC staining and imaged by Leica confocal microscopy. (B) Plumbagin inhibited VEGF-induced cofilin phosphorylation in HUVECs using immunofluorescences staining with specific antibody for phosphorylated cofilin. photographs labelled VEGF + plumb were from the group treated with 5 μM plumbagin. (C) Plumbagin inhibited VEGF-induced VEGFR2 phosphorylation in a dose-dependent manner in HUVECs. (D) Plumbagin suppressed the VEGF-induced activity of Ras and Rac1 (GTP-bound form) in the pull-down assay and decreased the phosphorylation level of their downstream proteins including PAK1, LIMK1, cofilin using specific antibodies in HUVEC cells. The grey analysis was shown in digital format located between the Western blot bands of total and activated forms of proteins.

together these results suggest that plumbagin exerts its effects upon cell migration by interference with the VEGFR2-mediated Ras/Rac1/cofilin pathway.

Plumbagin blocks Ras/MAPK pathway in HUVECs

Data from the MTS proliferation assay (Figure 4D left) showed an inhibitory effect of plumbagin on HUVEC proliferation. We then employed Western blotting to detect the phosphorylation levels of essential proteins in the MAPK pathway mediated by Ras. Our results showed that plumbagin produced a dose–dependent inhibition of VEGF-stimulated phosphorylation of MEK, ERK and JNK. These results confirmed our hypothesis that plumbagin inhibited HUVEC proliferation via blocking the Ras/MAPK pathway.

Discussion

Plumbagin is a small (MW 188) bioactive compound frequently found in plant extracts listed in the TCMM and has been shown to exert many biological actions (Premakumari *et al.*, 1977; Santhakumari *et al.*, 1978; Krishnaswamy and Purushothaman, 1980; Luo *et al.*, 2010). However, no previous studies have examined the effects of plumbagin on angiogenesis, especially tumour angiogenesis. In this study, we have demonstrated that plumbagin inhibited tumour growth and tumour angiogenesis both *in vitro* and *in vivo* Moreover, inhibition of tumour angiogenesis by plumbagin was due to its effects upo the VEGF-induced Ras/Rac/cofilin and Ras/MAPK signalling pathways.

Tumour angiogenesis is pivotal for tumour growth and metastasis. In this study, we showed that plumbagin slowed the growth of human HCT116 colon tumour and PC-3 prostate tumour growth in xenograft mouse tumour models without causing discernable side effects (Figures 3 and 4). In addition, we also performed P65 over-expression experiments in HUVEC, and results showed that, in the absence of plumbagin, the P65 over-expression group showed more obvious pro-proliferative effects under higher doses of X-ray exposure, which substantiated the role of P65 in radioresistance (Figure S2). Our results suggested that endothelial cell and tumour angiogenesis may be the important aspects of anti-tumour activity by plumbagin.

VEGF and its high-affinity receptor VEGFR-2 are the most widely studied factors in angiogenesis (Sandur *et al.*, 2006). Targeting of VEGFR-2 is an intriguing strategy in the anti-angiogenic therapy of tumours. In this investigation, we identified plumbagin as an inhibitor of VEGF-induced VEGFR2 phosphorylation and activation (Figure 5C), suggesting that VEGFR2 is a potential target of plumbagin in the process of inhibiting of tumour angiogenesis and tumour growth in endothelial cells.

In the VEGF/VEGFR2-mediated angiogenic cascade, Ras-mediated signalling pathways are of significance (Rak and Kerbel, 2001). Some members of small GTPases, such as Rac1 and RhoA, are engaged in actin polymerization, cytoskeletal rearrangement and cell migration (Barnes *et al.*, 2005). Previous studies had shown that Rac1 regulated lamellipodia formation (Sells *et al.*, 1999) and also functioned upstream of RhoA (Sander *et al.*, 1999) which itself controlled cell actin stress fibre formation (Van Aelst and D'Souza-Schorey, 1997). However, later studies (Guo *et al.*, 2006) showed that the deletion of Rac1 also abolished actin stress fibres in the cells without detectable alteration of endogenous RhoA activity. Rac1 is also essential for actin stress fibre formation independent of RhoA activity; rather, RhoA appears to require functional Rac1 for stress fibre induction. This observation may explain our findings that plumbagin disrupted VEGF-induced actin stress fibre formation (Figure 5A) and hampered Rac1 activity, while having little effect upon RhoA activity (Figure 5D). This suggested that the impairment of stress fibre formation by plumbagin involved Rac1 rather than RhoA. , Rac-1 itself causes the activation of PAK1, resulting in the consequent activation of LIMK1 and cofilin (Ishizaki *et al.*, 1997; Edwards *et al.*, 1999), which in turn promotes the formation of stress fibres, actin polymerization and cell migration (Starinsky-Elbaz *et al.*, 2009). In this study, we found that plumbagin dramatically down-regulated VEGF-induced cofilin activity using immunofluorescence and Western blotting (Figure 5B and D). Furthermore, we also found that plumbagin hampered VEGF-induced phosphorylation and activation of PAK1, LIMK1, and cofilin using Western blotting (Figure 5D). Taken together with the *in vitro* data in the migration assays (Figure 1B and C), we suggest that plumbagin inhibited cytoskeleton reorganization and stress fibre formation and hence cell migration through suppression of the VEGFR2-mediated Ras/Rac/cofilin pathway.

In addition to the regulation of Ras on cell migration, the Ras/MEK/ERK pathway also governs the signalling networks that control cell proliferation and survival (Kolch, 2000). Our results also demonstrated that plumbagin limited the VEGF-induced activity of MEK, ERK and JNK in a dose-dependent manner (Figure 6A). In addition, we also tested the effects of plumbagin on FGF-induced ERK phosphorylation activity of HUVEC. Our results showed that plumbagin did not inhibit FGF-induced ERK phosphorylation at concentrations which act upon the VEGF-VEGFR2 pathway (data not shown).

Integrating the results of HUVEC proliferation and migration assays, the present study suggested that the Ras signalling pathway was essential in the modulation of tumour angiogenesis by plumbagin (Figure 6B).

In conclusion, our results have shown that plumbagin is a novel suppressor of angiogenesis and should be evaluated in diseases where angiogenesis is a major contributor to the pathology.

Acknowledgements

This study is partially sponsored by The Pujiang Program (09PJ1403900) and the Research Platform for Cell Signalling Networks (06DZ22923) from the Science and Technology Commission of Shanghai Municipality (M Liu) and by grants from the National Natural Science Foundation of China (30971523, 81071807) (Z Yi); Major State Basic Research Development Program of China (2009CB918402) (Z Yi) and PhD Program Scholarship Fund of ECNU 2008 (2010045) (Y Dong).

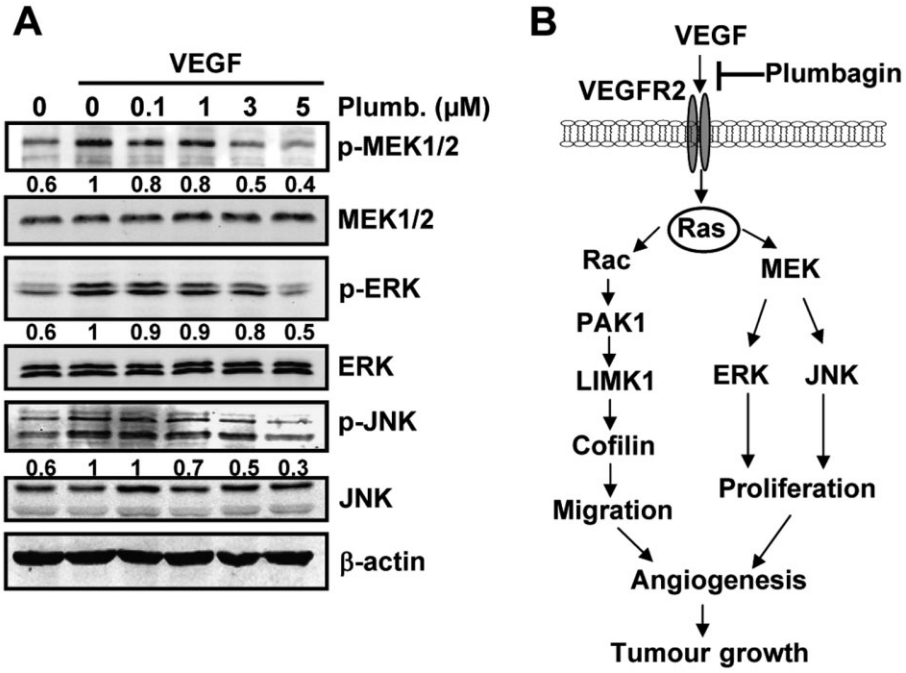

Figure 6

(A) Plumbagin inhibited VEGF-induced MEK, ERK and JNK phosphorylation using Western blotting analysis; 40 ng protein of the whole cell lysate was loaded and run on 10–12% SDS-PAGE. Phosphorylated MEK, phosphorylated ERK and phosphorylated JNK were detected by specific antibodies. The grey analysis was shown in digital format located between the Western blot bands of total and activated forms of proteins. (B) Proposed model for how plumbagin represses tumour angiogenesis through Ras signalling pathways in endothelial cells. Based on the inhibition of VEGFR2 activation, plumbagin may inhibit endothelial cell migration by affecting Ras downstream cascade of the Ras–Rac–cofilin pathway. In addition, plumbagin may suppress endothelial cell growth by acting on the Ras-mediated cascade of the Ras/MEK/ERK and Ras/MEK /JNK pathways.

Conflicts of interest

None.

References

Alexander SPH, Mathie A, Peters JA (2011). Guide to Receptors and Channels (GRAC). 5th edn. Br J Pharmacol 164 (Suppl. 1): S1–S324.

Barnes WG, Reiter E, Violin JD, Ren XR, Milligan G, Lefkowitz RJ (2005). beta-Arrestin 1 and Galphaq/11 coordinately activate RhoA and stress fiber formation following receptor stimulation. J Biol Chem 280: 8041–8050.

Bos JL, Fearon ER, Hamilton SR, Verlaan-de Vries M, van Boom JH, van der Eb AJ *et al.* (1987). Prevalence of ras gene mutations in human colorectal cancers. Nature 327: 293–297.

Cabebe E, Wakelee H (2006). Sunitinib: a newly approved small-molecule inhibitor of angiogenesis. Drugs Today 42: 387–398.

Carmeliet P, Jain RK (2000). Angiogenesis in cancer and other diseases. Nature 407: 249–257.

Checker R, Sharma D, Sandur SK, Khanam S, Poduval TB (2009). Anti-inflammatory effects of plumbagin are mediated by inhibition of NF-kappaB activation in lymphocytes. Int Immunopharmacol 9: 949–958.

Cho SG, Yi Z, Pang X, Yi T, Wang Y, Luo J *et al.* (2009). Kisspeptin-10, a KISS1-derived decapeptide, inhibits tumor angiogenesis by suppressing Sp1-mediated VEGF expression and FAK/Rho GTPase activation. Cancer Res 69: 7062–7070.

Dancey JE (2002). Agents targeting ras signaling pathway. Curr Pharm Des 8: 2259–2267.

Dong Y, Lu B, Zhang X, Zhang J, Lai L, Li D *et al.* (2010). Cucurbitacin E, a tetracyclic triterpenes compound from Chinese medicine, inhibits tumor angiogenesis through VEGFR2-mediated Jak2-STAT3 signaling pathway. Carcinogenesis 31: 2097–2104.

Dzoyem JP, Tangmouo JG, Lontsi D, Etoa FX, Lohoue PJ (2007). In vitro antifungal activity of extract and plumbagin from the stem bark of Diospyros crassiflora Hiern (Ebenaceae). Phytother Res 21: 671–674.

Edwards DC, Sanders LC, Bokoch GM, Gill GN (1999). Activation of LIM-kinase by Pak1 couples Rac/Cdc42 GTPase signalling to actin cytoskeletal dynamics. Nat Cell Biol 1: 253–259.

Eikesdal HP, Sugimoto H, Birrane G, Maeshima Y, Cooke VG, Kieran M *et al.* (2008). Identification of amino acids essential for the antiangiogenic activity of tumstatin and its use in combination antitumor activity. Proc Natl Acad Sci USA 105: 15040–15045.

Guo F, Debidda M, Yang L, Williams DA, Zheng Y (2006). Genetic deletion of Rac1 GTPase reveals its critical role in actin stress fiber formation and focal adhesion complex assembly. J Biol Chem 281: 18652–18659.

Hanrahan EO, Kies MS, Glisson BS, Khuri FR, Feng L, Tran HT *et al.* (2009). A phase II study of Lonafarnib (SCH66336) in patients with chemorefractory, advanced squamous cell carcinoma of the head and neck. Am J Clin Oncol 32: 274–279.

Hoa M, Davis SL, Ames SJ, Spanjaard RA (2002). Amplification of wild-type K-ras promotes growth of head and neck squamous cell carcinoma. Cancer Res 62: 7154–7156.

Huang Y, Chen X, Dikov MM, Novitskiy SV, Mosse CA, Yang L *et al.* (2007). Distinct roles of VEGFR-1 and VEGFR-2 in the aberrant hematopoiesis associated with elevated levels of VEGF. Blood 110: 624–631.

Ishizaki T, Naito M, Fujisawa K, Maekawa M, Watanabe N, Saito Y *et al.* (1997). p160ROCK, a Rho-associated coiled-coil forming protein kinase, works downstream of Rho and induces focal adhesions. FEBS Lett 404: 118–124.

Kane RC, Farrell AT, Saber H, Tang S, Williams G, Jee JM *et al.* (2006). Sorafenib for the treatment of advanced renal cell carcinoma. Clin Cancer Res 12: 7271–7278.

Karp JE, Flatten K, Feldman EJ, Greer JM, Loegering DA, Ricklis RM *et al.* (2009). Active oral regimen for elderly adults with newly diagnosed acute myelogenous leukemia: a preclinical and phase 1 trial of the farnesyltransferase inhibitor tipifarnib (R115777, Zarnestra) combined with etoposide. Blood 113: 4841–4852.

Kenyon BM, Voest EE, Chen CC, Flynn E, Folkman J, D'Amato RJ (1996). A model of angiogenesis in the mouse cornea. Invest Ophthalmol Vis Sci 37: 1625–1632.

Kobayashi M, Nishita M, Mishima T, Ohashi K, Mizuno K (2006). MAPKAPK-2-mediated LIM-kinase activation is critical for VEGF-induced actin remodeling and cell migration. EMBO J 25: 713–726.

Kolch W (2000). Meaningful relationships: the regulation of the Ras/Raf/MEK/ERK pathway by protein interactions. Biochem J 351: 289–305.

Kranenburg O, Gebbink MF, Voest EE (2004). Stimulation of angiogenesis by Ras proteins. Biochim Biophys Acta 1654: 23–37.

Krishnaswamy M, Purushothaman KK (1980). Plumbagin: a study of its anticancer, antibacterial & antifungal properties. Indian J Exp Biol 18: 876–877.

Lee CH, Lee HS (2008). Acaricidal activity and function of mite indicator using plumbagin and its derivatives isolated from Diospyros kaki Thunb. roots (Ebenaceae). J Microbiol Biotechnol 18: 314–321.

Luo Y, Mughal MR, Ouyang TG, Jiang H, Luo W, Yu QS *et al.* (2010). Plumbagin promotes the generation of astrocytes from rat spinal cord neural progenitors via activation of the transcription factor Stat3. J Neurochem 115: 1337–1349.

Meadows KN, Bryant P, Pumiglia K (2001). Vascular endothelial growth factor induction of the angiogenic phenotype requires Ras activation. J Biol Chem 276: 49289–49298.

Meadows KN, Bryant P, Vincent PA, Pumiglia KM (2004). Activated Ras induces a proangiogenic phenotype in primary endothelial cells. Oncogene 23: 192–200.

Morgan MA, Ganser A, Reuter CW (2007). Targeting the RAS signaling pathway in malignant hematologic diseases. Curr Drug Targets 8: 217–235.

Neal CP, Berry DP, Doucas H, Manson MM, Steward W, Garcea G (2006). Clinical aspects of natural anti-angiogenic drugs. Curr Drug Targets 7: 371–383.

Pang X, Yi T, Yi Z, Cho SG, Qu W, Pinkaew D *et al.* (2009). Morelloflavone, a biflavonoid, inhibits tumor angiogenesis by targeting rho GTPases and extracellular signal-regulated kinase signaling pathways. Cancer Res 69: 518–525.

Parikh C, Subrahmanyam R, Ren R (2007). Oncogenic NRAS, KRAS, and HRAS exhibit different leukemogenic potentials in mice. Cancer Res 67: 7139–7146.

Premakumari P, Rathinam K, Santhakumari G (1977). Antifertility activity of plumbagin. Indian J Med Res 65: 829–838.

Rak J, Kerbel RS (2001). Ras regulation of vascular endothelial growth factor and angiogenesis. Methods Enzymol 333: 267–283.

Rousseau S, Houle F, Kotanides H, Witte L, Waltenberger J, Landry J *et al.* (2000). Vascular endothelial growth factor (VEGF)-driven actin-based motility is mediated by VEGFR2 and requires concerted activation of stress-activated protein kinase 2 (SAPK2/p38) and geldanamycin-sensitive phosphorylation of focal adhesion kinase. J Biol Chem 275: 10661–10672.

Sander EE, ten Klooster JP, van Delft S, van der Kammen RA, Collard JG (1999). Rac downregulates Rho activity: reciprocal balance between both GTPases determines cellular morphology and migratory behavior. J Cell Biol 147: 1009–1022.

Sandur SK, Ichikawa H, Sethi G, Ahn KS, Aggarwal BB (2006). Plumbagin (5-hydroxy-2-methyl-1,4-naphthoquinone) suppresses NF-kappaB activation and NF-kappaB-regulated gene products through modulation of p65 and IkappaBalpha kinase activation, leading to potentiation of apoptosis induced by cytokine and chemotherapeutic agents. J Biol Chem 281: 17023–17033.

Santhakumari G, Rathinam K, Seshadri C (1978). Anticoagulant activity of plumbagin. Indian J Exp Biol 16: 485–487.

Saxena BP, Thappa RK, Tikku K, Sharma A, Suri OP (1996). Effect of plumbagin on gonadotrophic cycle of the housefly, Musca domestica L. Indian J Exp Biol 34: 739–744.

Sells MA, Boyd JT, Chernoff J (1999). p21-activated kinase 1 (Pak1) regulates cell motility in mammalian fibroblasts. J Cell Biol 145: 837–849.

Sharma I, Gusain D, Dixit VP (1991). Hypolipidaemic and antiatherosclerotic effects of plumbagin in rabbits. Indian J Physiol Pharmacol 35: 10–14.

Son TG, Camandola S, Arumugam TV, Cutler RG, Telljohann RS, Mughal MR *et al.* (2010). Plumbagin, a novel Nrf2/ARE activator, protects against cerebral ischemia. J Neurochem 112: 1316–1326.

Starinsky-Elbaz S, Faigenbloom L, Friedman E, Stein R, Kloog Y (2009). The pre-GAP-related domain of neurofibromin regulates cell migration through the LIM kinase/cofilin pathway. Mol Cell Neurosci 42: 278–287.

Van Aelst L, D'Souza-Schorey C (1997). Rho GTPases and signaling networks. Genes Dev 11: 2295–2322.

Yi T, Cho SG, Yi Z, Pang X, Rodriguez M, Wang Y *et al.* (2008a). Thymoquinone inhibits tumor angiogenesis and tumor growth through suppressing AKT and extracellular signal-regulated kinase signaling pathways. Mol Cancer Ther 7: 1789–1796.

Yi T, Yi Z, Cho SG, Luo J, Pandey MK, Aggarwal BB *et al.* (2008b). Gambogic acid inhibits angiogenesis and prostate tumor growth by suppressing vascular endothelial growth factor receptor 2 signaling. Cancer Res 68: 1843–1850.

Yi ZF, Cho SG, Zhao H, Wu YY, Luo J, Li D *et al*. (2009). A novel peptide from human apolipoprotein(a) inhibits angiogenesis and tumor growth by targeting c-Src phosphorylation in VEGF-induced human umbilical endothelial cells. Int J Cancer 124: 843–852.

Supporting information

Additional Supporting Information may be found in the online version of this article:

Figure S1 Plumbagin inhibits the proliferation of endothelial cells and tumour cells. (A) HUVEC, HCT116 and PC3 cells were labelled with BrdU after 0 or 3 μM plumbagin treatment for 24 h. (B) Quantitative data of percent of BrdU immunoreactive cells at indicated concentrations.

Figure S2 P65 over-expression in HUVEC. The pLVX-IRES-ZsGreen1 vector was used to over-expression p65 within lentivirals in HUVECs. P65 was amplified by PCR from p65 plasmid using the following primers: 5′-CGCTCGAGATGGACGAACTGTTCCCCCTC-3′ (sense), 5′-GCTCTAGATTAAGCGTAATCTGGAACATCGTATGGGTACATGGAGCTGATCTGACTCAG-3′ (antisense). After transfecting the p65-Zsgreen vector and control vector into the 293T cells, the virus-containing medium was harvested. HUVECs were infected with the virus for 24 h and then were cultured in normal ECM medium for 24 h and were re-infected for another 24 h. Then, the infected HUVECs were seeded into the 98-well plates at the density of 5000 cells per well. When adhered to the plates, cells were pretreated with 0, 1 or 3μM of plumbagin for 1 h followed by X-ray radiation at the dose of 0, 1, 5 or 10 Gy; 72 h later, the cell viability was measured by MTS assay.

Please note: Wiley-Blackwell are not responsible for the content or functionality of any supporting materials supplied by the authors. Any queries (other than missing material) should be directed to the corresponding author for the article.